

## Elaboration and rheological characterization of nanocomposite hydrogels containing C<sub>60</sub> fullerene nanoplatelets

Théo Merland<sup>1,2</sup>, Mathieu Berteau<sup>1</sup>, Marc Schmutz<sup>3</sup>, Stéphanie Legoupy<sup>4</sup>, Taco Nicolai<sup>1</sup>, Lazhar Benyahia<sup>1</sup>, Christophe Chassenieux<sup>1</sup>

<sup>1</sup> Institut des Molécules et Matériaux du Mans, UMR CNRS 6283, Le Mans Université, Avenue Olivier Messiaen, 72085 Le Mans Cedex 9, France

<sup>2</sup> Soft Matter Sciences and Engineering, ESPCI Paris, PSL University, Sorbonne University, CNRS, F-75005 Paris, France

<sup>3</sup> Université de Strasbourg, CNRS, Institut Charles Sadron, UPR 22, 23 Rue du Loess, 67034 Strasbourg Cedex, France

<sup>4</sup> Univ Angers, CNRS, MOLTECH-ANJOU, F-49000 Angers, France

### SUPPORTING INFORMATION.

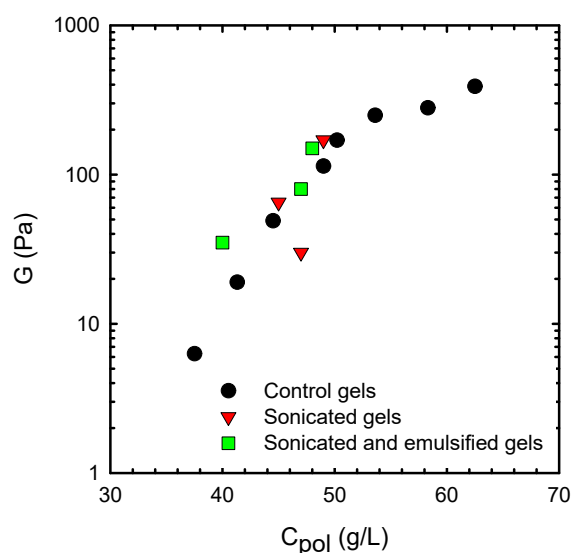


**Figure S1.** Shear modulus measured at  $T=20^{\circ}\text{C}$ ,  $\omega=10$  rad/s and  $\gamma=1\%$  for neat 75C12 hydrogels (black circles), gels sonicated during 8 minutes (red triangles) and gels sonicated during 8 minutes in the presence of 40 vol% carbon disulfide, that eventually completely evaporated (green squares).

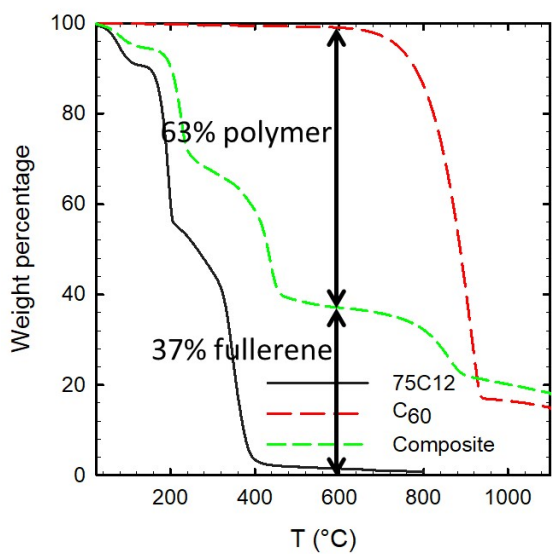


**Figure S2.** TGA thermogram obtained on freeze-dried powders for 75C12, C<sub>60</sub> and their composite with 63% polymer and 37% fullerene.

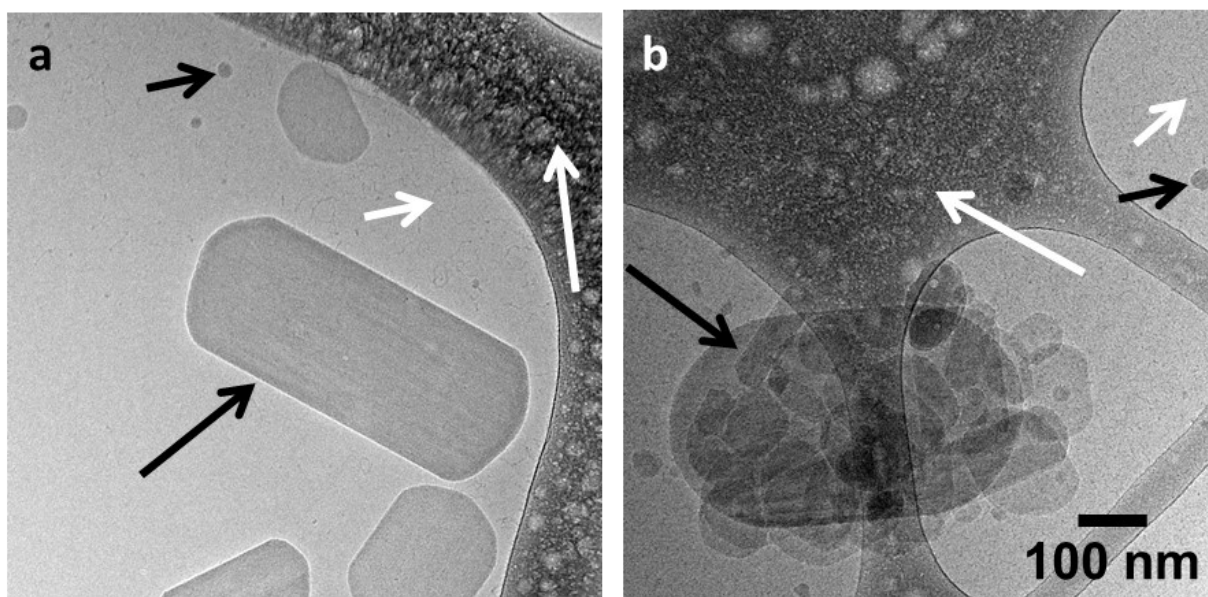


**Figure S3.** Enlarged representative cryo-TEM pictures of C<sub>60</sub> nanoplatelets dispersion in water before (a) and after redispersion following their freeze drying (b). Short white arrows show micelles (spherical + worm-like) formed by self-assembly of 75C12; long white arrows show the carbon-lacey supporting membrane; long black arrows show fullerene nanoplatelets; short black arrows show isotropic fullerene nanoparticles.

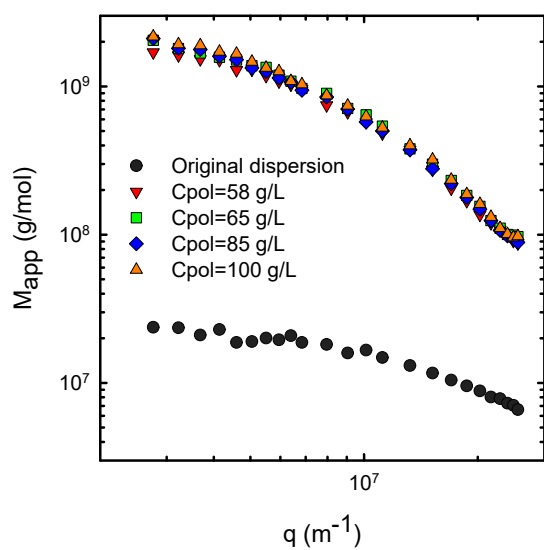


**Figure S4.** Apparent mass-weighted molar mass obtained by SLS for a dispersion of  $C_{60}$  nanoplatelets (black circles) and their re-dispersions in water at different concentrations as indicated in legend.

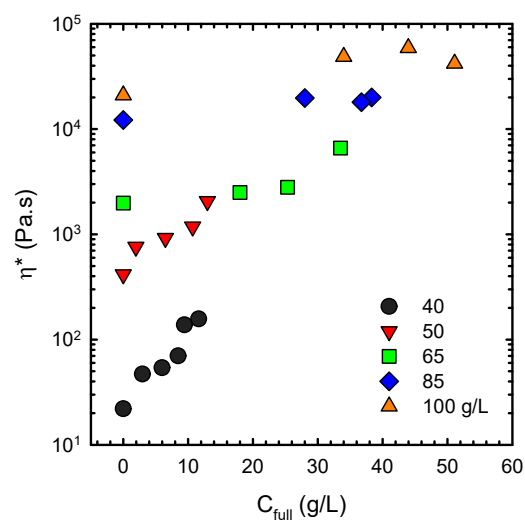


**Figure S5.** Evolution of complex viscosity upon fullerene concentration for hydrogels with various polymer concentrations as indicated in legend.

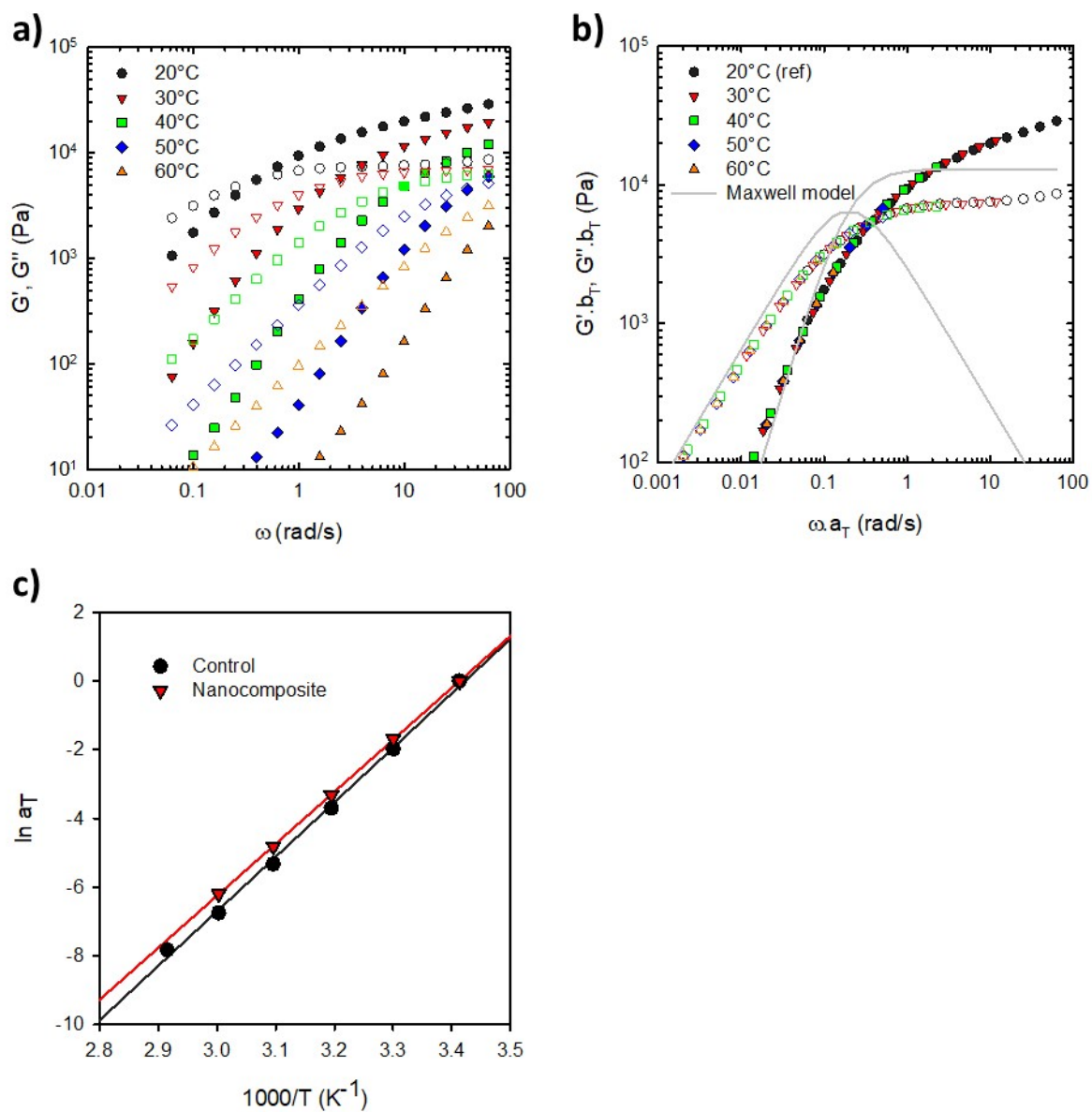


**Figure S6.** a) Storage ( $G'$ , close symbols) and loss ( $G''$ , open symbols) moduli as a function of frequency ( $\omega$ ) for a hydrogel with  $C_{pol}=100$  g/L and  $C_{fill}=51$  g/L measured at various temperature as indicated in the figure. b) Master curve of the same rheological data using 20°C as reference. The gray solid line is a Maxwell model with  $G=10$  kPa and  $\tau=3$ s. c) Arrhenius plot for the same hydrogel and a control sample with  $C_{pol}=100$  g/L.

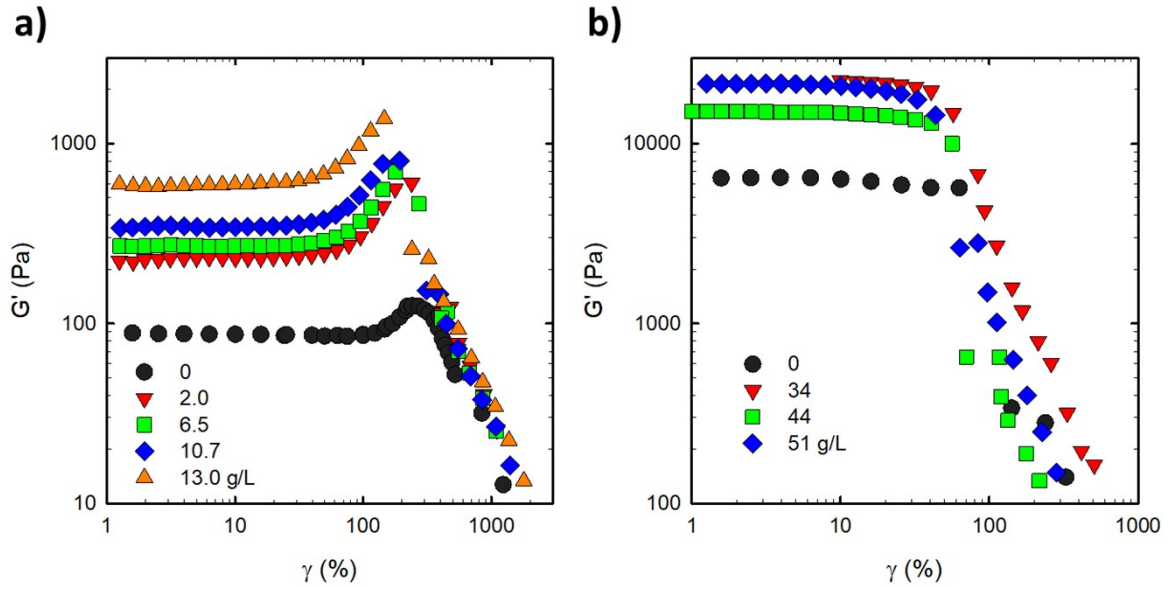


**Figure S7.**  $G'$  and  $G''$  as a function of strain for hydrogels with  $C_{pol} =$  a) 50 g/L and b) 100 g/L and various fullerene concentrations indicated in legend, at  $T=20^\circ\text{C}$  and  $\omega=10$  rad/s.

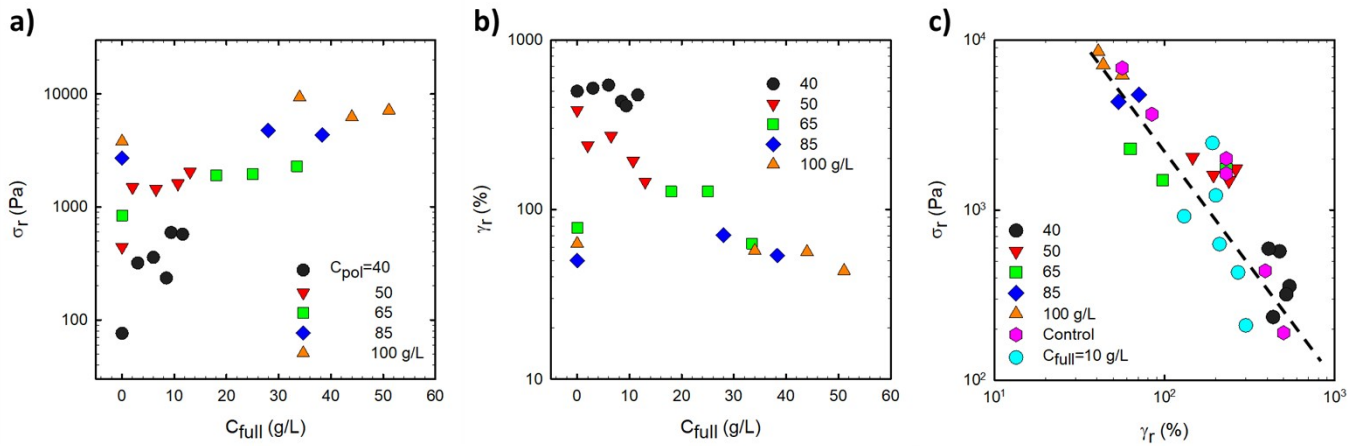


**Figure S8.** a) Stress and b) strain at rupture as a function of fullerene concentration with various  $C_{pol}$  as indicated in legend. c) Stress at rupture vs strain at rupture. Dashed line displays a power law with an exponent equal to  $-3/2$ .